

Cell-Free Massive MIMO in the O-RAN Architecture: Cluster and Handover Strategies

Robbert Beerten, Vida Ranjbar, Andrea P. Guevara, Sofie Pollin

Abstract

Recently, the O-RAN architecture started receiving significant interest from the research community. The open interfaces and especially the possibilities for network-wide control protocols via the Near-Real Time RAN Intelligent Controller provide a significant amount of opportunities to implement newly proposed algorithms from state-of-the-art research. O-RAN follows the trend towards disaggregation of network functionalities which is especially interesting to deploy Cell-Free Massive MIMO in realistic distributed networks. Many attractive solutions have been proposed for the physical layer in Cell-Free Massive MIMO networks. Unfortunately, only limited work has been performed to map these solutions to the Next Generation of Radio Access Networks, especially also considering the existing control plane interfaces and the impact on network-level resource allocation and handover. In this work, we propose a realistic and elegant method of modelling the temporal evolution of the channel in cell-free Massive MIMO. We then build clustering and handover strategies and provide numerical results for multiple deployment scenarios. To realistically evaluate handovers and dynamic clustering for cell-free in O-RAN, we consider a fixed clustering strategy, which computes the ideal cluster whenever a handover threshold is exceeded, and an opportunistic clustering strategy, where serving units are added opportunistically as the user moves. Additionally, we map an uplink detection method from the current cell-free Massive MIMO state-of-the-art to the O-RAN architecture. We study how the ageing of the channel and especially the user-centric cluster around the UE limits the performance of Cell-Free algorithms. We identify what is currently possible and propose the few needed extensions to O-RAN to fully exploit state-of-the-art cell-free processing schemes.

Index Terms

Cell-Free Massive MIMO, Distributed Processing, Next-Generation Radio Access Networks, Scalable Implementation, Dynamic Clustering

This research has received funding from the European Union’s Horizon 2020 research and innovation programme under Grant Agreement No. 101017171 (MARSAL project).

I. INTRODUCTION

The next generation of wireless networks will require enormous data rates. To this end, many solutions have been promised, Cell-Free Massive MIMO (CF mMIMO) being amongst the most popular ones. It has been studied thoroughly by many researchers [1] since its initial conception [2]. On the other hand, O-RAN only recently gained significant traction in the research community. we show considerable synergy between these two and demonstrate that their combination has the ability to enable the next generation of wireless networks.

A. *O-RAN*

Recently, O-RAN has emerged as a way to organise mobile networks. This new architecture proves to be interesting for practical deployments of CF mMIMO networks for two reasons. First, the physical layer is split between the O-RAN Distributed Units (O-DUs) and Radio Units (O-RUs). Second, extra functional blocks are introduced, enabling AI and containerised service orchestration on the network. These include the Near-Real Time RAN Intelligent Controller (Near-RT RIC), the Non-RT RIC, and the Service Management and Orchestration (SMO) framework [3]. The new interfaces and options for network-wide control can be exploited to achieve cooperation amongst O-RUs, even beyond the borders of the O-DUs. This work will focus on how an O-RAN network can achieve cooperation and smooth handover between its O-DUs via our proposed inter-O-DU interface, the E2 interface, and xApps in the Near-RT RIC. An xApp is a function in the Near-RT RIC which optimises the network via the E2 interface. The authors of [4] demonstrate a typical use-case for an xApp, which is network-wide handover management for load balancing and interference management in a cellular network. The reader is referred to [5] for an overview of the O-RAN architecture.

B. *Cell-Free Massive MIMO*

CF mMIMO refers to a network with many more Access Points (APs) than User Equipment (UEs), where APs cooperate via coherent joint transmission and reception. Numerous promising algorithms have been proposed, many of which target the physical layer [6]–[8]. However, a good deal of questions remain unanswered in resource scheduling, including pilot allocation, power control, and user clustering. And especially, it is unknown how to organise these networks practically and which changes and extensions to current standards are required to let APs cooperate optimally. [9] proposes a way to integrate CF mMIMO into the Cloud-RAN (C-RAN) architecture

while optimising for energy efficiency. The optimisation problem is tailored specifically towards a C-RAN deployment. They split the total power consumption into parts for Optical Network Units, APs, and DUs in the cloud. An initial attempt at standardisation of cooperation across APs was made in the LTE standard via Coordinated Multipoint Joint Transmission (CoMP-JT). Unfortunately, the standard never became very clear, especially regarding how exactly those cooperating APs should organise their transmissions and how they should coordinate amongst APs. The main problem was limited interest from system vendors since legacy APs could only achieve marginal gains from the cooperative serving of UEs [10]. CF mMIMO attempts to overcome this by utilising algorithms from Massive MIMO in TDD, densely deployed networks and user-centric transmission [11]. User-centric clustering was already identified as an important research direction for CoMP networks [12]. Many seminal works discuss a Central Processing Unit (CPU) which is responsible for the higher parts of the physical layer processing. The centralisation of all computations in a central unit should be avoided as this imposes immense requirements on the fronthaul capacity and computing power of that singular unit. The idea of the CPU not being one single entity already exists for a relatively long time and is explored in [13]–[16]. The authors in [13] claim that the CPU should not be thought of as a physically central unit but as a collection of algorithms that can be run anywhere in the network. [14] proposes an architecture where multiple CPUs cooperate to serve its UEs via user-centric clustering. They propose an algorithm with performance comparable to the canonical, ubiquitous cell-free case while being scalable. This idea is reflected in our work, where O-DUs decode the signal collaboratively. The Near-RT RIC serves as an additional network-wide controller which executes specific optimisation algorithms.

C. State of the Art in Mobility Modeling

The current temporal models for CF mMIMO are rather limited. [17]–[20] use the Jakes autocorrelation model, where the different channels are assumed to be from the same distribution, and the autocorrelation is modelled via a Bessel function. In [21], the UE moves along a predetermined straight line. Their mmWave channel consists of an LoS component and an NLoS component, both are updated at discrete sampling times. The location of the UE determines the AoA and the path loss; thus, the LoS component can be computed directly. The NLoS components are computed as an autoregressive function via the Jakes autocorrelation model. They primarily focus on beamforming that is more robust to UEs mobility. In [22], the probability

of handover in Network MIMO is studied using distance-based metrics. As such, they do not model the channel itself but only the movement of the UEs. [23] uses a blockage map of an urban location; hence, the shadowing is consistent between UEs and along the path of the UE. This is interesting as it mimics real-life shadowing very closely, although it does not account for moving blockers. Unfortunately, it is computationally very taxing and scenario-dependant. They also use the concept of soft handover, but they are more focused on pilot allocation.

D. Synergy between O-RAN and Cell-Free

The O-RAN Alliance builds upon the continuing trend of increased disaggregation and soft-warisation in the RAN. This trend has already passed three uniquely identifiable stages: 1) Distributed RAN (D-RAN) has the BBU and the RRH both at the cell site; 2) Cloud RAN (C-RAN) [24] collocates the BBUs at a shared pool; 3) Virtual RAN (vRAN) [25] decouples the software from the hardware by implementing parts of the RAN as standalone software components. 3GPP has determined a range of physical layer splits (1-8) [26] where more functions are moved to the BBU with an increasing split number. Conversely, the RRH becomes more simplistic with increasing split number [27]. O-RAN, which uses split 7.2x, is just one example of these possible functional splits per 3GPP's specifications. The disaggregation of the RAN is also an essential aspect of implementing cell-free networks. The theoretical CF literature emphasises this strongly. In most seminal CF papers [28], [29] the APs are quite cheap and mostly responsible for the channel estimation and, in the case of Large-Scale Fading Decoding (LSFD), for computing a local signal estimate [11]. Numerous works in theoretical CF have discussed how the functional split should be made between an AP and the CPU [30].

We see great value in mapping the current state-of-the-art CF mMIMO research onto the O-RAN architecture. The Central Processing Unit (CPU) can be disaggregated into the Near-RT RIC and a set of cooperating O-DUs. Cooperation between distributed APs has previously been proposed in many scenarios under different terms such as CoMP-JT, D-MIMO, CF, and so on. At this point in the development of the O-RAN architecture, it is vital to identify and select the most significant contributions from these many different topics. A first physical layer-focused mapping between CF mMIMO and O-RAN was proposed in [31] where the joint computation of a precoder is studied across both O-RAN Radio Units (O-RUs) and O-DUs. They conclude that not only enabling cooperation between O-RUs but also between as many O-DUs as possible is the best approach in terms of spectral efficiency. Unfortunately, a high degree of cooperation

requires significant computing power and signalling capacity between the O-DUs due to the large amounts of channel state information (CSI) needed to calculate the precoder. In this paper, we extend this mapping by also considering user mobility; thus, the allocation of O-DUs and O-RUs to a UE should change, resulting in a full or partial handover.

E. Contributions

In a practical CF mMIMO network, it is practical and realistic to assume coherent combining only at the AP [32]–[34]. This greatly simplifies implementation costs and makes it possible to achieve CF mMIMO with minor changes to the O-RAN architecture, as detailed in this paper. This motivates us to use a local decoder at every O-RU and then combine based on large-scale changes; hence we choose the method from [35]. In [31], it was also shown that inter-DU cooperation leads to great benefits.

- We propose how to map an Uplink (UL) detection method [35] to the O-RAN framework and combine this with the new concepts of measurement and serving clusters. For this mapping, we further detail the information exchange across the relevant existing interfaces between O-RU, O-DU and Near-RT RIC and build upon the work from [36].
- We propose a way to evolve the channel temporally in CF mMIMO. This method evolves the large-scale fading of the channel only. Thus, it allows studying the impact of the large-scale fading in the channel on cluster update algorithms operating over large time intervals.
- We propose two clustering and handover strategies and quantify their performance via our selected UL detection method. We detail how initial clusters could be determined and how the serving cluster can be updated based on a trigger by the user or opportunistically based on information locally available for each O-RU. Subsequently, we map these to the O-RAN framework and discuss the signalling flow over the existing E2 interface.

F. Outline

First, we define our clustering strategies in Section II. In Section III, we give an overview of our CF mMIMO system model and extend it to allow for temporal evolution. Subsequently, in Section IV, we provide handover strategies for the clustering strategies in Section II. Finally, in Section V, we map all of the previous to the O-RAN architecture and provide practical guidelines on how they could be implemented with minimal changes to O-RAN. In Section VI, we give numerical results for the proposed solutions.

G. Notation

A diagonal matrix with the elements x_i on the main diagonal is denoted by $\text{diag}(x_0, x_1, \dots, x_N)$. The cardinality of a set \mathcal{S} is written as $|\mathcal{S}|$. For matrices and vectors alike, \mathbf{A}^T is the transpose, \mathbf{A}^H is the Hermitian conjugate of the matrix, and \mathbf{A}^* is the complex conjugate. The l 'th element of vector \mathbf{a} is denoted by $[\mathbf{a}]_l$. The expected value of x is denoted by $\mathbb{E}\{x\}$. We also list our commonly used symbols in Table I.

TABLE I: List of symbols

Symbol	Definition	Symbol	Definition
K	Total number of UEs	C	Number of O-DUs
L	Total number of O-RUs	N	Number of antennas per O-RU
$\hat{\mathbf{h}}_{l,k}$	Estimated channel vector between UE k and O-RU l	$\mathbf{h}_{l,k}$	Channel Vector between UE k and O-RU l
$\beta_{l,k}[t]$	Channel Gain between UE k and O-RU l at time t	$\beta_{l,k}^{\text{dB}}[t]$	Channel gain between UE k and O-RU l at time t expressed in dB
$\mathcal{M}_k^s[t]$	Serving Cluster for UE k at time t	\mathcal{M}_k^m	Measurement Cluster for UE k
$O_k[t]$	Function that selects best O-RUs from measurement cluster for UE k at time t	$Q_l^{(w)}[t]$	Function that selects w best UEs for O-RU l at time t
l_k^*	Index of primary O-RU for UE k	K_l^*	Number of UEs that use O-RU l as primary O-RU
\mathbf{a}_k	LSFD combiner for UE k	$\mathbf{v}_{l,k}$	Receive combiner for UE k in O-RU l
\mathcal{D}_l	Set of UEs that are served by O-RU l	p_k	UL power of UE k
$\mathbf{R}_{l,k}$	Covariance matrix of channel between UE k and O-RU l	$\mathbf{C}_{l,k}$	Channel estimation error covariance matrix between UE k and O-RU l
\mathcal{P}_k	Set of UEs that share the pilot with UE k	τ_p	Length of the pilot sequence
ϕ_{t_k}	Pilot sequence with index t_k	\mathbf{n}_l	Received noise vector at O-RU l
s_k	Symbol transmitted by UE k	$\hat{s}_{l,k}$	Estimate for received signal from UE k at O-RU l
g_{ki}	Effective gain for UE i in the combining vector for UE k	$F_{l,k}[t]$	Shadow fading between UE k and O-RU l at time t

II. CLUSTER FORMATION

In this section, we define two clustering strategies for determining the set of O-RUs that serve a UE. To define the two clustering strategies, we introduce the concepts of *primary O-DU* and *O-RU, measurement cluster* and *serving cluster*. When a UE first connects to the network, that UE chooses a primary O-RU, and the O-DU that controls that O-RU logically becomes

the primary O-DU. Physical layer processing is split between O-RU and O-DU, i.e. the O-RU applies the combining vector; the O-DU computes the combining vector, estimates the channel and combines the decoded signal from O-RUs based on large-scale fading coefficients. The concept of the primary O-RU (and O-DU) is important in our network, as the primary O-RU determines:

- **Handover:** The handover, as described in Section IV, occurs when a new primary O-RU is selected.
- **Measurement cluster:** The measurement cluster is a set of O-RUs located in proximity to the primary O-RU. With the primary O-RU, the measurement cluster is uniquely defined.

Two **Serving cluster** strategies are proposed in this section: a *Fixed* serving cluster formation and an *Opportunistic* serving cluster formation. The first one is fixed each time the UE triggers a handover. With such handover, a new primary O-RU and measurement cluster is determined, and a serving cluster is statically defined by the Near-RT RIC based on the reported channel gain measurements. The second method allows each O-DU, doing the channel estimation for its O-RU in the measurement cluster for a particular UE, to locally decide if any of those O-RUs should aid the signal decoding for the considered UE. Below, we detail the procedures for selecting the primary O-RU and measurement cluster and the two serving cluster formation methods. In this work, we assume the UL and DL to be completely power-reciprocal.

A. Primary O-RU and Measurement Cluster

Upon connection to the network, a UE instantiates a connection to a single O-RU and O-DU combination. This can be done via a procedure as outlined in [13]. In short, this method implies that a UE determines which O-RU provides the best channel gain towards the UE via a Downlink (DL) control signal. The UE then connects to this primary O-RU and its O-DU. Based on the primary O-RU location, the Near-RT RIC will then form a measurement cluster of O-RUs, \mathcal{M}_k^m , for that specific UE k . The goal of the measurement cluster is to limit the number of O-RUs on which the channel gain should be measured for a specific UE when determining the serving cluster. The serving cluster is a subset of O-RUs \mathcal{M}_k^s that aid in the joint precoding/decoding for a specific UE k . Note that these O-RUs can belong to one or multiple O-DUs, thus, potentially requiring O-DUs to cooperate. In this work, we take the measurement cluster to be the set of $|\mathcal{M}_k^m|$ O-RUs that are located the closest to the primary O-RU. We take the size of the measurement cluster to be twice as large as the serving cluster, i.e. $|\mathcal{M}_k^m| = 2|\mathcal{M}_k^s|$. The size of

the serving cluster is a network-wide parameter. The measurement cluster is the same for every method we discuss later and is uniquely defined by the primary O-RU location. Every O-DU that controls an O-RU $l \in \mathcal{M}_k^m$ is then notified that it should track the channel gain, $\beta_{l,k}$ for that specific UE k in the relevant O-RUs streams. In Section III-E, we explain how the large-scale fading in the channel is modelled as a function of UE mobility. Thus the access procedure, including the measurement cluster allocation, can be summarised as follows:

- 1) A UE completes an initial access procedure to the primary O-DU that controls the primary O-RU from which the UE has the highest DL channel gain $\beta_{l,k}$.
- 2) The primary O-DU requests the Near-RT RIC to designate a measurement cluster for the newly attached UE.
- 3) The Near-RT RIC designates a set of O-RUs as a measurement cluster, \mathcal{M}_k^m , for a specific UE; The O-DUs that control these O-RUs track the received power of the pilots of these UEs in the relevant O-RUs' streams.

This measurement cluster allows us to define two methods for finding a serving cluster which we will discuss in Subsections II-B and II-C. In this work, we employ two clustering strategies, fixed clustering and opportunistic tracking, and compare them against two baselines, ubiquitous CF and a cellular system with only the primary O-DU serving.

B. Fixed Cluster Formation

Algorithm 1 Initial Fixed Serving Cluster Formation

```

1: for  $k = 1 \dots K$  do
2:    $l_k^* = \arg \max_l \beta_{l,k}[0]$ 
3:    $\mathcal{M}_k^s[0] \leftarrow O_k[0]$ 
4:    $\bar{P}_k \leftarrow 10 \log_{10} \left( \sum_{l \in \mathcal{M}_k[0]} \beta_{l_k^*,k}[0] \right)$ 
5: end for

```

After the measurement clustered is obtained, the O-DUs that control O-RUs in the measurement cluster report the UL channel gains, $\beta_{l,k}$, for UE k to the Near-RT RIC. In Algorithm 1 we show how the fixed serving cluster is formed for a specific UE k by the Near-RT RIC. The $|\mathcal{M}_k^s|$ O-RUs with the highest UL channel gain are added to the serving cluster, and a metric \bar{P}_k , the sum of DL channel gains from the serving cluster to UE k , is determined. This metric

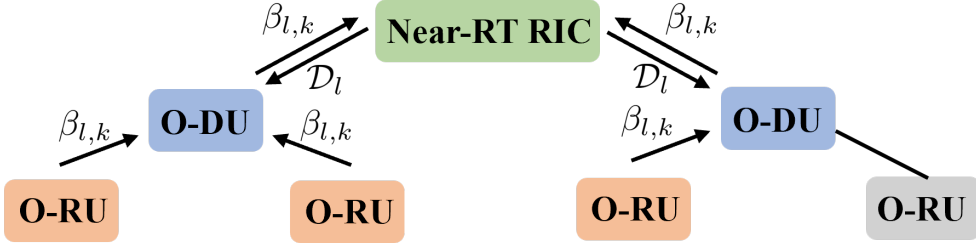


Fig. 1: Signalling Flow for the Fixed Clustering; Upon trigger by a UE, the O-DUs which control O-RUs in the measurement cluster (orange) measure the channel gain $\beta_{l,k}$ in the received stream from those O-RUs. The O-DUs then transfer these channel gains to the Near-RT RIC. The Near-RT RIC then notifies the O-DUs of the set of UEs, \mathcal{D}_l , to be served on each O-RU l .

represents the total signal quality in the cluster when it is created. This metric is also updated regularly from channel estimates and used by the handover mechanism, which will be discussed in Section IV. We define $O_k[t]$ as the function that maps the set of all O-RUs in the measurement cluster to a serving cluster which contains only the $|\mathcal{M}_k^s|$ O-RUs that experience the highest UL channel gains from that UE at time t . The main advantage of this method is that the number of O-RUs, $|\mathcal{M}_k^s|$, can be chosen by the Near-RT RIC. The main disadvantage is the large amount of signalling between the O-DUs and the Near-RT RIC.

C. Opportunistic Cluster Formation

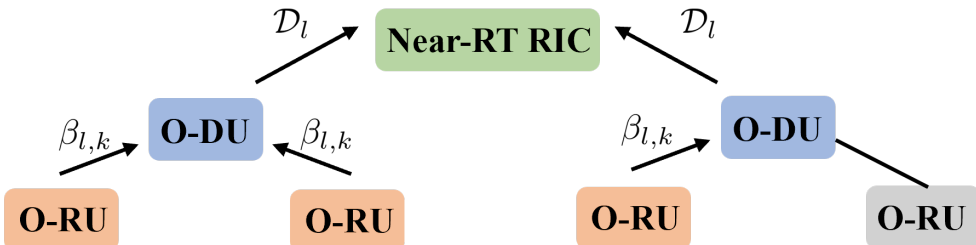


Fig. 2: Signalling flow for the Opportunistic Clustering; the O-DUs which control O-RUs in the measurement cluster (orange) measure the channel gain $\beta_{l,k}$ in the received stream from those O-RUs. The O-DUs can locally decide which UEs should be served on its O-RUs. The O-DU then notifies the Near-RT RIC of this set of UEs, \mathcal{D}_l , for each of its O-RUs.

By this method, after the allocation of the primary O-RU, primary O-DU and measurement cluster, the O-DUs can decide locally if they serve a specific UE on O-RUs that have unused resources without involving the Near-RT RIC. O-DUs decide opportunistically by only selecting the UEs with the highest UL channel gains. Since O-DUs can decide autonomously, we need a way to limit the size of the serving cluster. We achieve this by having both a limited measurement cluster and placing an upper limit on the number of UEs that a specific O-RU can serve opportunistically. By this method, we attempt to only select the best UEs per O-RU. This is a different approach to achieving the same goal of a limited number of O-RU serving each UE in the fixed clustering scheme. In the fixed clustering approach, the Near-RT RIC selects the best O-RUs for a specific UE and the serving cluster has a deterministic size. In the opportunistic approach, the O-DU selects the best UEs for each O-RU and the size of the serving cluster is upper bounded by the number of UEs per O-RU and the size of the measurement cluster. Algorithm 2 shows how the O-RUs can be loaded maximally.

In contrast to the fixed clustering strategy, this opportunistic strategy avoids a network-wide procedure executed at the Near-RT RIC. We define \mathcal{D}_l as the set of all UEs that are served by O-RU l . The number of UEs that are selected for an O-RU has an upper limit, which we design here to be the number of antennas on the O-RU, N . Naturally, we let the UEs that use an O-RU as a primary take priority over those served opportunistically by the same O-RU. We define the function $Q_l^{(w)}[t]$ as the function that maps all the UEs whose measurement cluster contains O-RU l to the subset of w UEs that achieve the best channel towards O-RU l at time instance t . This function loads an O-RU up to its limit, including the UEs that use it as a primary O-RU i.e. an O-RU that can serve N UEs and currently serves K_l^* UEs as primary O-RU could take an additional $N - K_l^*$ UEs opportunistically. Notice the importance of the measurement cluster to the number of O-RUs that serve a specific UE, as only O-RUs in its measurement cluster can potentially be used to serve that UE. [37] also proposes an opportunistic clustering scheme where O-RUs can decide locally if they serve a specific UE. However, they base this decision on pilot contamination and do not consider UE mobility. The main advantage of this method is the low computational cost and load on the E2 interface. The only required signalling is the notification of the measurement clusters from the Near-RT RIC to the O-DUs. This message can also indicate which O-DU serves as the primary O-DU for a specific UE. This way, an O-DU knows with which O-DU it should instantiate inter-O-DU interfaces to enable cooperative decoding. The main disadvantage of this method is that there are no guarantees on the number

Algorithm 2 Initial Opportunistic Cluster Formation

```

1: for  $k = 1 \dots K$  do
2:   Assign O-RU with highest gain to each UE (primary O-RU)
3:    $l_k^* = \arg \max_l \beta_{l,k}[0]$ 
4: end for
5: for  $l = 1 \dots L$  do
6:   For each O-RU, add more UEs up to the maximum of  $N$ 
7:    $\mathcal{D}_l[0] \leftarrow Q_l^{(N-K_l^*)}[0]$ 
8:    $\bar{\beta}_{l,k}^{\text{dB}} \leftarrow \beta_{l,k}^{\text{dB}}[0] \quad \forall k \in \mathcal{D}_l$ 
9: end for

```

of serving O-RUs beyond the primary O-RU.

D. Ubiquitous Cell-Free

By this method of operation, every UE is served by every single O-RU in the network and thus $|\mathcal{M}_k^s| = L$. We use this as an upper bound on the performance of the clustering. It is expected that performance drops when only part of the network is used to serve a specific UE. By comparing to the optimal, ubiquitous case, we can evaluate the performance gap to a heuristic handover scheme.

E. Cellular

In the cellular case, every UE is served only by O-RUs connected to a single O-DU. Hence, only $|\mathcal{M}_k^s| = L/C$ O-RUs cooperate to serve a single UE. Thus, the cellular case is used as a lower bound on the performance to show the benefits of implementing our proposed inter-O-DU interface. The disadvantages are two-fold; first the amount of O-RUs is inherently limited due to the size of the O-DU, second, the set is never optimal as there is a high probability that O-RUs from a different O-DU might have a better channel to the UE than the selected O-RUs. This method of operation is similar to canonical Distributed MIMO.

III. SYSTEM MODEL

This section describes how to tackle UL detection, channel estimation, and combiner calculation during a specific coherence block. We use a method from the current state-of-the-art

and map it to the O-RAN architecture. Most of subsections III-A, III-B, and III-C are adapted from [38]. In Section III-E, we extend our system to allow for mobility of the UEs and how to temporally evolve our channel model. Section IV then discusses how the clusters should be reformed based on the mobility of the UEs.

A. Channel Model

In this work, we consider UL detection. We assume each O-RU to have N antennas, the channel vector between a single-antenna UE k and an O-RU l is thus defined as $\mathbf{h}_{l,k} \in \mathbb{C}^N$. We assume $\mathbf{h}_{l,k}$ to be from a complex normal distribution,

$$\mathbf{h}_{l,k} \sim \mathcal{CN}(\mathbf{0}, \mathbf{R}_{l,k}), \quad (1)$$

where $\mathbf{R}_{l,k} \in \mathbb{C}^{N \times N}$ is the covariance matrix of the channel. This model implies that we assume the channels between one UE and different O-RUs to be mutually uncorrelated. This is a valid assumption if the O-RUs are placed many wavelengths apart. We assume these $\mathbf{R}_{l,k}$ to be known at their respective O-RU l and the respective O-DU. Some methods exist to estimate these from a relatively limited amount of samples [39]. We will later link these $\mathbf{R}_{l,k}$ to our mobility model in Section III-E. We simulate a system with K UEs, L O-RUs, C O-DUs and a single Near-RT RIC. The O-DUs are placed in a uniform grid; in each square in this grid there are L/C O-RUs; these O-RUs are placed randomly via a uniform random distribution.

B. Channel Estimation

To estimate the channel, the UEs transmit mutually orthogonal pilot sequences $\phi_i \in \mathbb{C}^{\tau_p}$. The O-DU can exploit this orthogonality to separate the UEs while estimating the channel. In the UL, UE k transmits pilot ϕ_{t_k} in the designated time slot, where t_k is the index of the pilot allocated to UE k . O-RU l receives the superposition of all of the UEs' pilots as $\mathbf{Y}_l \in \mathbb{C}^{N \times \tau_p}$:

$$\mathbf{Y}_l = \sum_{k=1}^K \sqrt{p_k} \mathbf{h}_{l,k} \phi_{t_k}^T + \mathbf{N}_l. \quad (2)$$

\mathbf{N}_l is a matrix with the measured noise realizations $\mathbf{n}_{t,l}$ in the columns. Each of its elements are i.i.d. distributed white noise from the distribution $\mathcal{CN}(0, \sigma_{\text{ul}}^2)$. The transmit power of UE k is p_k . The O-DU can estimate the respective channels per O-RU as these O-RUs are assumed to be many wavelengths apart and thus the channels between a specific UE and multiple O-RUs are mutually uncorrelated. The O-DU decorrelates these received pilots for UE k in O-RU l as

$\mathbf{y}_{l,k}^{(p)} = \mathbf{Y}_l \frac{\phi_{t_k}^*}{\sqrt{\tau_p}}$. Afterwards, only interference from UEs that share the same pilot remains, which is known as pilot contamination [40]. UEs that share their pilot with UE k are denoted via the set \mathcal{P}_k . The decorrelated pilot simplifies to,

$$\mathbf{y}_{l,k}^{(p)} = \sum_{i \in \mathcal{P}_k} \sqrt{p_i \tau_p} \mathbf{h}_{l,i} + \mathbf{N}_l \phi_{t_k}^*. \quad (3)$$

The O-DU then calculates the MMSE channel estimates between UE k and O-RU l , $\hat{\mathbf{h}}_{l,k}$, as

$$\hat{\mathbf{h}}_{l,k} = \sqrt{\tau_p p_k} \mathbf{R}_{l,k} \left(\sum_{i \in \mathcal{P}_k} \tau_p p_i \mathbf{R}_{l,i} + \sigma_{\text{ul}}^2 \mathbf{I}_N \right)^{-1} \mathbf{y}_k^{(p)}. \quad (4)$$

We denote the error on the channel estimate as

$$\tilde{\mathbf{h}}_{l,k} = \hat{\mathbf{h}}_{l,k} - \mathbf{h}_{l,k}. \quad (5)$$

The covariance of this channel estimation error is $\mathbf{C}_{l,k}$.

C. Receive Combining

Nearly-Optimal Large-Scale Fading Decoding (n-opt LSFD) fits nicely into the O-RAN architecture. We employ this decoding scheme by having the primary O-DU calculate the n-opt LSFD weights [28] based on the effective gains in all of the O-RUs of the serving clusters. UL detection has three stages in our system. First, each O-RU l estimates the signal $\hat{s}_{l,k}$ of its served UEs, $k \in \mathcal{D}_l$, locally and sends these local estimates to its respective O-DU. Second, this O-DU c computes more accurate estimates for the UE's signal \hat{s}_k^c based on the LSFD weights of the UE's signal, \hat{s}_k^c , to their respective primary O-DU which combines them into the final estimate for the UE's signal, \hat{s}_k . This combination at the secondary and primary O-DUs is organized such that we reach the n-opt LSFD solution in the primary O-DU for the final decoding step. This mapping of n-opt LSFD to the O-RAN architecture and the division of computations between what we call primary and secondary O-DUs was proposed in [36]. The interface between two cooperating O-DUs is a concept which was explored in [31], [36]. The received signal at each O-RU is,

$$\mathbf{y}_l = \sum_{k=1}^K \mathbf{h}_{l,k} s_k + \mathbf{n}_l. \quad (6)$$

In our analysis, we use the Local Partial MMSE (LP-MMSE) combiner [13] as it is computed separately for each O-RU. The fronthaul specification in O-RAN [41] supports both transfer of the receive combining vector from the O-DU to the O-RU over the fronthaul as well as transfer

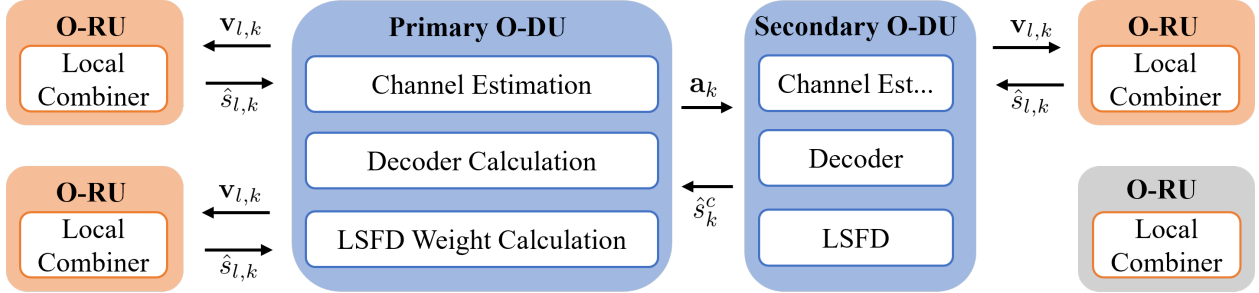


Fig. 3: Overview of the O-DU/O-RU and the inter-O-DU signalling required for the cooperative detection. We show both the signalling between O-RU and O-DU and the inter-O-DU signalling. On the left (primary) O-DU both O-RUs are used in decoding, on the right (secondary) O-DU, only the top O-RU is used.

of CSI to the O-RU such that the O-RU can calculate the combining vector itself. Here, we assume the first option. The O-DU computes an LP-MMSE receive combiner $\mathbf{v}_{l,k}$ for each of its O-RU - UE associations,

$$\mathbf{v}_{l,k} = p_k \left(\sum_{i \in \mathcal{D}_l} p_i \left(\hat{\mathbf{h}}_{l,i} \hat{\mathbf{h}}_{l,i}^H + \mathbf{C}_{l,i} \right) + \sigma_{ul}^2 \mathbf{I}_N \right)^{-1} \hat{\mathbf{h}}_{l,k}. \quad (7)$$

This is where the signal processing is linked to the serving clusters \mathcal{M}_k^s from Section II. The O-DU computes this combiner only if $k \in \mathcal{D}_l$. The O-RU then locally combines the received signal via $\mathbf{v}_{l,k}$ for all the UEs that it serves as

$$\hat{s}_{l,k} = \mathbf{v}_{l,k}^H \mathbf{y}_{l,k}, \quad \forall l \in \mathcal{M}_k^s. \quad (8)$$

We compute cluster-wide LSFD combining weights for the local O-RU estimates. \mathbf{g}_{ki} is the effective gain for UE i in the receive combiner for UE k and $\delta_{l,k}$ indicates if UE k is served by O-RU l ,

$$\mathbf{g}_{ki} = \begin{bmatrix} \delta_{1,k} \mathbf{v}_{1,k}^H \mathbf{h}_{1,i} & \delta_{2,k} \mathbf{v}_{2,k}^H \mathbf{h}_{2,i} & \dots & \delta_{L,k} \mathbf{v}_{L,k}^H \mathbf{h}_{L,i} \end{bmatrix}^T. \quad (9)$$

We denote the set of UEs that share at least one O-RU with UE k as \mathcal{S}_k . In n-opt LSFD, it is assumed that only those UEs in \mathcal{S}_k induce significant interference for UE k , and thus we only cancel interference from those UEs. The primary O-DU can calculate the n-opt LSFD weights $\mathbf{a}_k \in \mathbb{C}^L$ as [35],

$$\mathbf{a}_k = p_k \left(\sum_{i \in \mathcal{S}_k} \mathbb{E}\{\mathbf{g}_{ki} \mathbf{g}_{ki}^H\} + \mathbf{F}_k \right)^{-1} \mathbb{E}\{\mathbf{g}_{kk}\}. \quad (10)$$

Where \mathbf{F}_k is defined as

$$\mathbf{F}_k = \sigma_{\text{ul}}^2 \text{diag}(\mathbb{E}\{\|\delta_{1,k} \mathbf{v}_{1,k}\|\}, \dots, \mathbb{E}\{\|\delta_{L,k} \mathbf{v}_{L,k}\|\}). \quad (11)$$

The weight vector for UE k , \mathbf{a}_k , has $|\mathcal{M}_k^s|$ non-zero elements, one for each O-RU that is serving UE k . The LSFD weights are only a function of the statistics of the channels and thus the secondary O-DUs do not need to pass any channel estimates to the primary O-DU. The statistics of different O-RUs are uncorrelated and thus the primary O-DU can combine the statistics of its own O-RUs and the O-RUs of secondary O-DUs without introducing any error [38]. The secondary O-DUs only need to give the primary O-DU timely updates of these channel statistics. We consider the relevant statistics to be known at the O-DU for each UE that is served by its' O-RUs. In this work we do not consider the updates of channel statistics to the primary O-DU and consider them perfectly known at the primary O-DU as well. We calculate the LSFD combining weights and possibly new clusters on the same timescale. At every timestep, we first check if a new cluster is needed, possibly update the cluster and then always update the LSFD weights. Future work should also consider updates of the LSFD weights based on a metric for the ageing of these weights without necessarily updating the cluster. From the primary O-DU to the secondary O-DU, the only signalling required are the relevant elements of \mathbf{a}_k to the O-RUs of this secondary O-DU which are in the serving cluster of UE k . We denote the set of O-RUs that are connected to O-DU c as \mathcal{L}_c . O-DU c can combine the signals locally for each UE served by O-RU $l \in \mathcal{L}_c$ as

$$\hat{s}_k^c = \sum_{l \in \mathcal{L}_c} [\mathbf{a}_k^*]_l \hat{s}_{l,k}. \quad (12)$$

The communication of these \mathbf{a}_k between O-DU is an extension from [36], we see it as an important part of this inter-O-DU interface. The primary O-DU then computes the final estimate for the UE's signal by combining the estimates of each of the serving O-DUs, \hat{s}_k^c .

$$\hat{s}_k = \sum_c \hat{s}_k^c = \sum_{l \in \mathcal{M}_k^s} [\mathbf{a}_k^*]_l \hat{s}_{l,k} \quad (13)$$

The result from (13) is the same solution as if a centralized CPU would compute the result via LSFD. Due to how the calculations are organised, the result is transparent to how the O-RUs are organized amongst the different O-DUs; after all, the n-opt LSFD weights are calculated per O-RU. In our proposed architecture, computations are divided amongst the primary O-DUs; thus enabling us to scale the algorithm across a large number of O-RUs and O-DUs.

D. Spectral Efficiency

$$\text{SINR}_k^{\text{ul}} = \frac{p_k |\mathbf{a}_k^H \mathbb{E}\{\mathbf{g}_{kk}\}|^2}{\mathbf{a}_k^H \left(\sum_{i \in \mathcal{S}_k} p_i \mathbb{E}\{\mathbf{g}_{ki} \mathbf{g}_{ki}^H\} - p_k \mathbb{E}\{\mathbf{g}_{kk}\} \mathbb{E}\{\mathbf{g}_{kk}^H\} + \mathbf{F}_k \right) \mathbf{a}_k} \quad (14)$$

From these previous equations, we can estimate the SINR as in (14) [35]. Via Equation 15, we can then estimate the spectral efficiency (SE) based on the SINR. This result is used in Section VI to show the performance of the clustering:

$$\text{SE}_k^{\text{ul}} = \log_2(1 + \text{SINR}_k^{\text{ul}}). \quad (15)$$

E. Proposed Long-term Evolution Mobility Model

Next, we explain how the channel model can be evolved temporally. The UEs move in a straight line from their starting position at a random angle $\theta_k \sim \mathcal{U}[0, 2\pi]$. The moving direction, θ_k , and the speed of the UE, v_k , are fixed for each simulation run. The sample time of the simulation is T_S . A UEs position at time t is then,

$$\begin{aligned} x[t] &= x[t-1] + v_k T_S \cos(\theta_k) \\ y[t] &= y[t-1] + v_k T_S \sin(\theta_k) \end{aligned} \quad (16)$$

If the deployment of O-RUs is dense, a minor movement of a UE could induce a significant change in the Angle of Arrival (AoA) for the received signal at an O-RU and thus change the covariance matrix of the channel significantly (see Eq. 19). Therefore, we do not expect the channel itself to be strongly correlated over multiple time samples, but we expect the large-scale fading to be correlated. Hence, we model shadow fading as an autoregressive function. From [42], it is known that the shadow fading at two points with distance d is correlated as $e^{-\alpha d}$, where α is the reciprocal of the decorrelation distance. We take α to be $\frac{1}{20\text{m}}$ in this example. This is the recommended value for a typical European city [42]. [43] indicates that the decorrelation distance becomes larger for more rural areas. We consider a relatively dense deployment of O-RUs, which is typical for an urban area, and thus our value for α is valid. We assume that the shadow fading follows the same distribution during our simulation. A UE moves a distance of $v_k T_S$ between two subsequent samples. Thus we can model the shadow fading $F_{l,k}[t]$ at any of the subsequent time intervals as

$$F_{l,k}[t] = \rho_k F_{l,k}[t-1] + \sqrt{1 - \rho_k^2} F_{l,k}^{\text{new}}. \quad (17)$$

Where $\rho_k = e^{-\alpha v_k T_S}$ is the correlation coefficient for two subsequent realizations, $F_{l,k}^{\text{new}}$ is a newly drawn shadow fading from the distribution $\mathcal{N}(0, \sigma_{\text{sf}}^2)$. Our model allows to have correlated shadow fading for different samples of a specific UE but not between different UEs. In the end, this leads to a path loss model which is constructed as

$$\beta_{l,k}^{\text{dB}}[t] = a + b \log_{10}(d_{l,k}[t]) + F_{l,k}[t]. \quad (18)$$

Where a is the path loss at the reference distance, b is the distance dependant path loss coefficient, $d_{l,k}$ is the distance between a specific UE k and O-RU l . The closest existing model is the one in [21] where the individual NLoS components are updated. In this work we update the shadow fading coefficient as a whole and evolve it using an empirically validated model.

Shadow fading plays an important role in the proposed solution because the measurement cluster is constructed by taking the closest O-RUs to the primary one. Since shadow fading occurs, the O-RUs that are closer to the UE might not be optimal as they could be (partially) blocked. O-RUs that are further away might provide a higher channel gain. Generally, the probability of further O-RUs being better than closer ones increases with increasing shadow fading variance. Although we have chosen a fixed measurement cluster, it might be valuable to make this size dependent on shadow fading variance. Because we consider a dense deployment of O-RUs, a relatively small movement of the UE might induce a big change in the angle of arrival for a particular UE - O-RU association. Hence, the channel covariance matrices should be regenerated at every new time instance. To calculate the second-order statistics of the channel, we use the one-ring scattering model [44] to calculate the elements of the covariance matrix,

$$[\mathbf{R}_{l,k}]_{m,n}[t] = \beta_{l,k}[t] \int e^{2\pi j d_H(n-m) \sin(\bar{\phi})} f(\bar{\phi}, t) d\bar{\phi}, \quad (19)$$

where $f(\bar{\phi}, t)$ is the time-dependent distribution of the possible angles of arrival. This distribution can be either Gaussian, Laplacian or uniform around the true angle of arrival for the signal. For this work, we consider a uniform distribution. In this case

$$\bar{\phi} = \phi + \delta, \quad \delta \sim U[-\xi, \xi], \quad (20)$$

where ϕ is the true angle of arrival, and ξ models the richness of the scattering environment.

IV. HANDOVER

If a serving cluster can only use a subset of the O-RUs in the network and we consider UE mobility, any selected subset of O-RUs will become suboptimal as the UE moves away from its

cluster. Hence, in this section, we propose updating strategies for the clusters from Section II. For the fixed clustering in Section II-B, we define a threshold for the entire cluster based on the DL power received at the UE. For the opportunistic cluster in Section II-C, we define a threshold per O-RU such that UEs select their primary O-RU and the O-DUs can decide locally which UEs to serve on which O-RUs opportunistically. We discuss these handover procedures at discrete times t , which are spaced apart at the same intervals, T_s , as in Section III-E.

A. Handover for Fixed Clustering

Algorithm 3 Handover for Fixed Clustering

```

1: Initialize:
2:    $\mathcal{M}_k^s[0] \leftarrow O_k[0]$ 
3:    $\bar{P}_k \leftarrow \sum_{l \in \mathcal{M}_k^s[0]} 10 \log_{10} (\beta_{l,k}[0])$ 
4: for  $t = 1 \dots T$  do
5:    $P_k[t] \leftarrow 10 \log_{10} \left( \sum_{l \in \mathcal{M}_k^s[t]} \beta_{l,k}[t] \right)$ 
6:   if  $\bar{P}_k - P_k[t] > M_{\text{HO}}^F$  then
7:      $\mathcal{M}_k[t] \leftarrow O_k[t]$ 
8:      $\bar{P}_k \leftarrow 10 \log_{10} \left( \sum_{l \in \mathcal{M}_k^s[t]} \beta_{l,k}[t] \right)$ 
9:   else
10:     $\mathcal{M}_k^s[t] \leftarrow \mathcal{M}_k^s[t - 1]$ 
11:   end if
12: end for

```

First, we describe a handover strategy for our fixed clustering strategy. In this case, the UE monitors the average received power $P_k[t]$, and triggers a handover if it is below the initial cluster power $\bar{P}_k - M_{\text{HO}}^F$, where M_{HO}^F is a hysteresis threshold. The threshold brings a trade-off in the system's performance (higher SE) versus less signalling overhead (less frequent handovers). When the UE triggers a handover, it selects a new primary O-RU with the highest DL channel gain. The new primary O-DU then requests a new measurement cluster around the new primary O-RU and, subsequently, a serving cluster for that UE from the Near-RT RIC. To keep track of the received power, we assume that in the DL control channel, the UE learns the DL channel gain from its O-RUs. Different works have argued in favour of DL pilots in CF mMIMO [45], and thus we see this as a valid assumption. It is also possible to transmit the UL measurements

back to the UE in a control channel and to use these under mild reciprocity assumptions. We provide pseudocode in Algorithm 3.

B. Opportunistic Cluster Tracking

Algorithm 4 UE Tracking in Opportunistic Clustering

```

1: for  $t = 1 \dots T$  do
2:   for  $k = 1 \dots K$  do
3:      $\bar{l} \leftarrow \arg \max_l \beta_{l,k}^{\text{dB}}$ 
4:     if  $(\beta_{\bar{l},k}^{\text{dB}}[t] > \beta_{l_k^*,k}^{\text{dB}}[t] + M_{HO}^O) \wedge (\bar{l} \neq l_k^*)$  then
5:       Primary O-RU handover
6:        $\mathcal{D}_{l^*}[t] \leftarrow Q_{l^*}^{(N-K_l^*+1)}[t]$ 
7:        $l_k^* \leftarrow \bar{l}$ 
8:        $\mathcal{D}_{\bar{l}}[t] \leftarrow Q_{\bar{l}}^{(N-K_{\bar{l}}^*)}[t]$ 
9:     end if
10:   end for
11:   for  $l = 1 \dots L$  do
12:     if  $\exists \bar{k} \notin \mathcal{D}_l[t] : \beta_{l,\bar{k}}^{\text{dB}}[t] > \beta_{l,k}^{\text{dB}}[t] + M_{HO}^O, \quad k \in \mathcal{D}_l[t]$  then
13:       Opportunistic O-RU Reload
14:        $\mathcal{D}_l[t] \leftarrow Q_l^{(N-K_l^*)}[t] \cup \{k : l_k^* = l\}$ 
15:     else
16:        $\mathcal{D}_l[t] \leftarrow \mathcal{D}_l[t-1]$ 
17:     end if
18:   end for
19: end for

```

We also define a handover strategy for our clustering with opportunistic tracking. In opportunistic tracking, the cluster updates on two different levels: 1) The primary O-RU; 2) The opportunistic serving by the O-DU. Every UE is connected to one O-RU as its primary one, denoted by l_k^* . A change of the primary O-RU requires the UE to perform an actual handover, hence we call this the *primary O-RU handover*. To limit the signalling between the O-DUs and the Near-RT RIC, it is logical to make the UE responsible for the handover of its primary O-RU as it is the UE's only persistent connection. A UE selects a new primary O-RU when it detects a

significantly higher DL channel gain to a different O-RU in its measurement cluster. If that UE makes its new primary O-RU exceed its limit of served UEs, that O-RU drops the weakest UE it is currently serving opportunistically. When the primary O-RU is updated, the measurement cluster changes accordingly, i.e. the closest O-RUs to the new primary O-RU become the new measurement cluster.

Additionally, the O-DUs can dynamically change the set of UEs it is opportunistically serving on its O-RUs. We call this an *opportunistic O-RU reload*. Once an O-DU detects a UE with a significantly higher UL channel gain than the UEs it is currently serving on one of its O-RUs, the serving set for that O-RU is updated opportunistically by the O-DU. The O-DU achieves this by selecting the UEs with that O-RU in their measurement cluster with the highest UL channel gains (via $Q_l^{(w)}[t]$ from Section II-C). Any changes in the opportunistic serving can happen dynamically as this does not change any connections between UEs and their primary O-RU. We introduce the handover threshold as M_{HO}^{O} and design it to be the same for the handover of the primary O-RU and the opportunistic addition of extra UEs. However, we do acknowledge that it might be interesting to use different thresholds for the primary handover and opportunistic O-RU reload. We outline the algorithm in Algorithm 4.

C. Ubiquitous

By this method, the UE is served by every O-RU in the system. The UE can move anywhere without significant losses because the LSFD combiner can calculate new combining weights \mathbf{a}_k based on the changing channel for every O-RU. Hence, there is no handover needed. However, it is helpful to highlight the performance gap to this method.

D. Cellular

By this method, a UE requests a handover when it detects that it has a significantly higher DL channel gain to an O-RU in a different O-DU than the one by which it is currently served. The threshold for this handover is M_{HO}^{C} . The algorithm is described in Algorithm 5.

V. INTEGRATION INTO O-RAN

The recent adoption of the O-RAN framework is a strong enabler for CF mMIMO networks. The disaggregation of the network and the introduction of the Near-RT RIC prove to be extremely useful in deploying CF mMIMO networks. This section expands on the discussion in our previous

Algorithm 5 Cellular Handover

```

1: for  $t = 1 \dots T$  do
2:   for  $k = 1 \dots K$  do
3:      $\bar{l} \leftarrow \arg \max_{l \notin \mathcal{M}_k^s} \beta_{l,k}^{\text{dB}}$ 
4:     if ( $\beta_{\bar{l},k}^{\text{dB}} > \beta_{l_k^*,k}^{\text{dB}} + M_{\text{HO}}^{\text{C}}$ ) then
5:        $\mathcal{M}_k^s[t] \leftarrow \{\mathcal{L}_c | \bar{l} \in \mathcal{L}_c\}$ 
6:     else
7:        $\mathcal{M}_k^s[t] \leftarrow \mathcal{M}_k^s[t - 1]$ 
8:     end if
9:   end for
10: end for
  
```

work [36]. We provide an overview of how our clustering (Section II) and handover (Section IV) strategies could be implemented with minimal changes to the O-RAN architecture. We focus on how the E2 interface and the Near-RT RIC can be used.

A. E2 - Service Models

The first important aspect is the E2 interface. It allows the Near-RT RIC to control its E2 nodes; we mainly consider the O-DUs as there is no E2 interface to the O-RUs. This control is implemented via so-called E2 Service Models (E2SMs) [46]. Currently, four E2SMs exist:

- Network Interface (E2SM-NI): monitors and modifies messages sent on 3GPP interfaces (S1, X2, NG, Xn, F1, E1).
- Key Performance Measurement (E2SM-KPM): monitors RAN and UE performance.
- RAN Control (E2SM-RC): monitors and modifies RAN parameters per UE.
- Cell Configuration and Control (E2SM-CCC): monitors and modifies RAN parameters per E2-node or cell.

The following paragraphs will indicate how we use the E2SM-KPM and E2SM-RC to enable our clustering and handover strategies.

B. Fixed Clustering and Handover

We first detail the usage of the E2 interface for the fixed clustering and handover strategy.

- 1) *Initial Access*; The UE connects to the network via its primary O-DU. This O-DU then requests a measurement cluster from the Near-RT RIC.
- 2) *Measurement Cluster Allocation*; The Near-RT RIC allocates the nearest O-RUs to the primary O-RU for that UE as a measurement cluster and signals this to the participating O-DUs. This notification can be sent via E2SM-KPM.
- 3) *Serving Cluster Allocation*; The participating O-DUs report the received power for the UE via the E2SM-KPM. This service model enables the Near-RT RIC to subscribe to UE-specific measurements. An xApp in the Near-RT RIC can then exploit these measurements to select the fixed cluster. The Near-RT RIC then signals, via the E2SM-KPM, to every O-DU that has any O-RUs in the serving cluster for that UE, the ID of the UE and the ID of the primary O-DU. This way, the secondary O-DUs know where to forward the partially decoded signals.
- 4) *Handover*; If the UE measures that its received power has deteriorated too much, it hands over to a new primary O-RU. The new primary O-DU notifies the Near-RT RIC, the Near-RT RIC then allocates a new measurement cluster and, subsequently, a new serving cluster.

The E2SM-KPM already supports performance monitoring per UE. Hence the way we intend to use it would only require minimal changes. The E2SM-RC, however, currently does not support the reporting of serving decisions to specific O-DUs. Especially the instantiating of inter-O-DU interfaces would require significant changes to the current specification.

C. Opportunistic Clusters

The signalling flow for the opportunistic approach is the same up until the point where the participating O-DUs are notified that they are in the measurement cluster.

- 2) *Measurement Cluster Allocation*; The measurement cluster for opportunistic clusters should be assigned via E2SM-RC as the O-DU is given (partial) autonomy on the decision of the serving cluster.
- 3) *Cluster Formation*; The participating O-DUs can decide locally on opportunistic serving. They only notify the Near-RT RIC if they decide to serve a certain UE on an O-RU. This can be achieved via the E2SM-KPM. This way the Near-RT RIC can notify O-DUs if they should instantiate or break inter-O-DU interfaces and to which O-DU they should forward

which signals in case there is a handover of the primary O-RU. This can be achieved via E2SM-RC.

- 4) *Primary O-RU Handover*; A UE measures a significantly better channel to an O-RU that is not its primary. It then signals its primary O-DU that it will handover to a different O-RU. The primary O-DU uses E2SM-KPM to notify the Near-RT RIC. The Near-RT RIC then notifies every O-DU that participates in the serving for that UE that it will get a different primary O-RU and O-DU. This notification can be sent over the E2SM-RC. Thus, the secondary O-DUs know where to forward the partially decoded signal.
- 5) *Opportunistic O-RU Reload*; The O-DU measures a significantly stronger UE than the weakest of the UEs it is currently serving on one of its O-RUs. It then triggers a new measurement on that O-RU to determine the strongest UEs. The O-DU signals to the Near-RT RIC which UEs it serves on that O-RU via the E2SM-KPM.

This method of operation requires very little input from the Near-RT RIC and it serves more as a bookkeeper that keeps track of which UEs are served by which O-RUs. The E2SM-RC should be extended to give a O-DU notice that it should involve a certain UE in its cluster formation. The E2SM-KPM should be extended to allow an O-DU to notify the Near-RT RIC that it is now serving a UE on certain O-RUs, one of them possibly being the primary one. The method would require minor changes to the E2SM-KPM and E2SM-RC. We argue that the potential benefits from the inter-O-DU cooperation outweigh the limited changes to the interface.

VI. SIMULATION AND NUMERICAL RESULTS

Parameter	Value	Parameter	Value	Parameter	Value
K	40	L	36	C	9
N	4	σ_{ul}^2	-94 dBm	Grid Size	1 x 1 km
Number of Setups	25	τ_p	100	T_s	0.5s
Simulation Time	10s	ξ	10°	\mathcal{M}_k^s	16

TABLE II: Simulation Parameters

We generate a scenario with K UEs and C O-DUs, L O-RUs and a single Near-RT RIC. The UEs are located in a square grid, this grid is divided into uniformly sized squares for each O-DU, the O-RUs for a specific O-DU are then placed randomly in the subsquare for its O-DU via a uniform distribution. We duplicate the initial setup eight times to create a wrap-around

scenario, so we have a configuration with 3×3 tiles and avoid performance differences between UEs in the centre and the edges of the centre tile.

A. Numerical Results

In this section, we quantify the performance of the different clustering methods. For the figures that relate to the clustering, we provide the canonical, ubiquitous cell-free case as an upper bound for the performance of our clustering/handover algorithms; because all O-RUs cooperate in this scenario. Additionally, we also provide the cellular case as a lower bound on the performance; for this case, we use a handover threshold of 2 dB. For the figures that are specific to the clustering methods, we use a decorrelation distance of 20m.

B. Decorrelation Distance

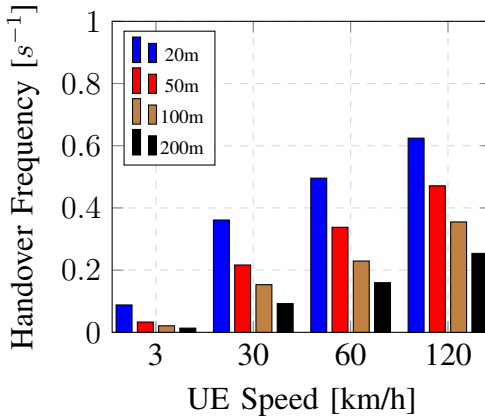


Fig. 4: Effect of the decorrelation distance $\frac{1}{\alpha}$ on the handover frequency of the cellular case for UEs travelling at various speeds

Figure 4 shows the effect of the chosen decorrelation distance in the proposed temporal channel model. When the decorrelation distance increases, handover occurs significantly less frequently. This occurs due to the shadowing fading remaining similar over longer distances. Note that doubling the speed and halving the decorrelation distance have almost the same effect. There is no effect on the SE because we estimate the SE at the same times the cluster is checked.

C. Fixed Clustering and Handover

Figure 5 shows the effect of the handover threshold on the distribution of the spectral efficiency for the fixed clustering and handover strategy. A lower handover threshold increases the handover

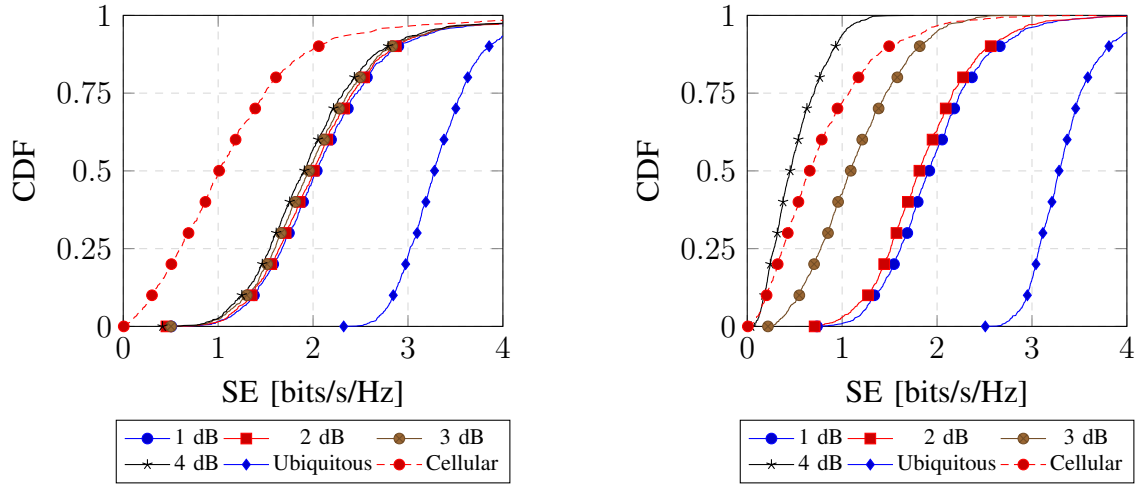


Fig. 5: Spectral Efficiency Distributions for UEs travelling at 30 km/h (left) and 120 km/h (right) for different HO thresholds for the fixed clustering and handover strategy

frequency; thus, on average, the serving O-RUs are of higher quality. However, this induces a considerable signalling cost because of the increased amount of handovers. For the fixed clustering, the Near-RT RIC calculates the cluster. Hence, we must be careful not to overload this component with too many cluster calculations. Figure 5 also displays the same CDF for a higher speed of the UE. We notice that the threshold becomes more critical when the speed is high. Interestingly, for the high-speed case, the performance is worse than cellular if the threshold is too high (4 dB). Also note that if we use ubiquitous CF mMIMO, the CDFs for low and high speed are almost the same. This is further supported by the findings in Figure 8.

D. Opportunistic Clustering

In this section, we provide numerical results for the opportunistic clustering approach. First, we look at the CDF of the SE for different handover thresholds for UEs travelling at both 30 km/h and 120 km/h. Figure 6 shows that for a low speed, the threshold does not significantly impact the performance. For high speed, however, the threshold substantially impacts the SE. Even for high handover thresholds, the opportunistic clustering strategy has a performance that is better than the cellular case. As the opportunistic tracking is decided locally, without involvement of the Near Real-Time RIC, this method finds a good balance between performance and cost.

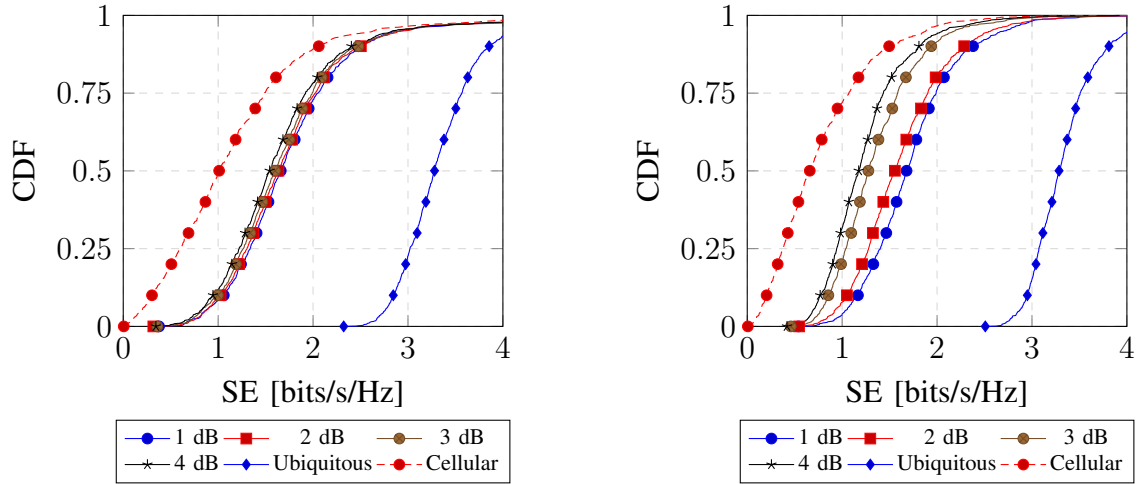


Fig. 6: Spectral Efficiency Distributions for UEs travelling at 30 km/h (left) and 120 km/h (right) for different HO thresholds for the opportunistic clustering and handover strategy.

E. Handover Frequency

Figure 7 quantifies the handover frequency for different speeds and different threshold values. Fixed clustering, which is expensive in terms of E2-signalling, has a lower handover frequency, even for a low threshold, than opportunistic clustering. Because, in the fixed case, the cluster-wide channel gain is tracked. This metric is less sensitive to the UE's mobility than the channel gain per O-RU. For both methods, the number of handovers increases with speed and decreases

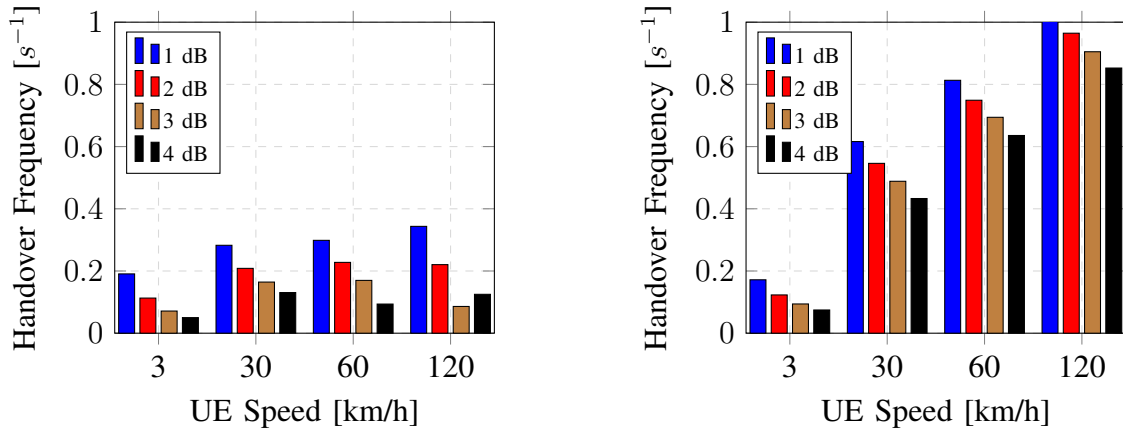


Fig. 7: Handover frequency for different thresholds M_{HO}^F for fixed clusters (right) and M_{HO}^O for opportunistic clusters (right).

with a rising threshold. This highlights a vital trade-off, a high frequency of handovers improves the SE significantly, especially for high speeds. For the fixed clusters, this becomes expensive as the E2 interface and the Near-RT RIC become more loaded. For opportunistic clustering, handover is relatively cheap as it does not require much signalling to the Near-RT RIC.

F. Comparison of Clustering Methods

Figure 8 shows the impact of the threshold on the SE as a function of speed for both the fixed and the opportunistic clustering strategies. For the fixed clustering, the mean SE drops with increasing UE speed. This effect is significant if the HO threshold is chosen too large. If the threshold is too large, performance degrades beyond that of the cellular case. The performance of the opportunistic clustering is less sensitive to the threshold value than the fixed clustering. This is because the UE only triggers the handover if the total received power decreases too much in the fixed clustering. The opportunistic clustering allows a new O-RU to easily start serving a new UE when that O-RU detects it as sufficiently strong. Hence, the opportunistic strategy provides more fine-grained control. This does, however, come at the price of not having a deterministic number of O-RUs that serve a particular UE and as such it is impossible for our algorithm to guarantee any quality of service beyond that provided by the primary O-RU. Furthermore, the ubiquitous case is barely affected by increasing speed of the UE.

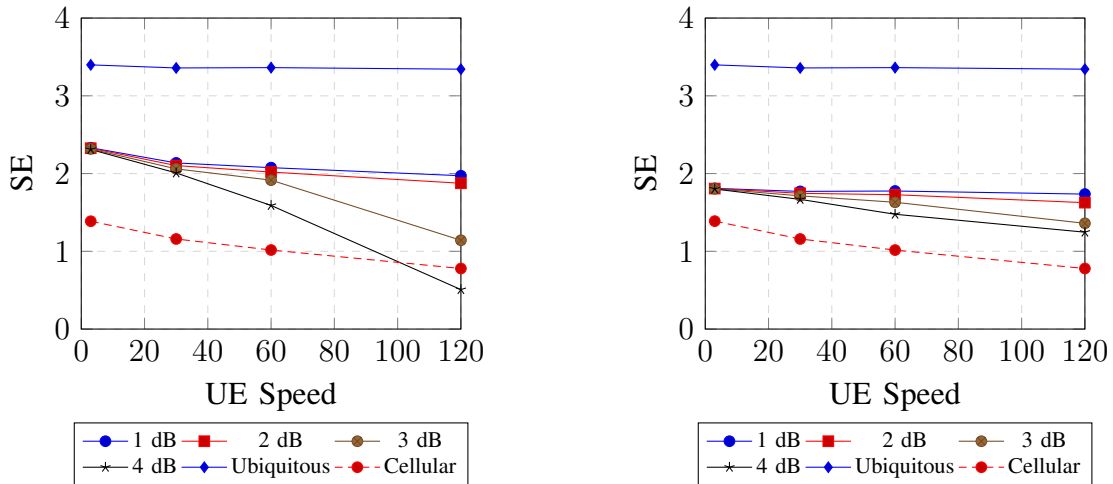


Fig. 8: Average SEs for UEs travelling at different speeds and for different HO thresholds for fixed clusters (left) and opportunistic clusters (right)

VII. CONCLUSION

In this work, we mapped an UL detection method from the CF mMIMO state-of-the-art to the O-RAN architecture. We proposed a temporal channel model based on the shadow fading for CF mMIMO and have shown its effect on handover frequency. We discussed two clustering and handover strategies, mapped them to the O-RAN architecture and benchmarked them via our selected UL detection method. We find that the opportunistic clustering works as well as the fixed clustering method and even better at high speeds and with significantly less signalling per handover. We also demonstrated that CF mMIMO is much more resilient against UE mobility than classical cellular systems (Figure 8). UE mobility in CF mMIMO is a research area still facing many complex problems, especially if user-centric clusters are considered instead of ubiquitous CF. We highlighted the significant synergy between O-RAN and the state-of-the-art in CF mMIMO and that O-RAN could be a strong enabler for CF mMIMO networks with only minimal changes to its architecture.

REFERENCES

- [1] E. Nayebi, A. Ashikhmin, T. L. Marzetta, and H. Yang, “Cell-free massive mimo systems,” in *2015 49th Asilomar Conference on Signals, Systems and Computers*, 2015, pp. 695–699.
- [2] H. Q. Ngo, A. Ashikhmin, H. Yang, E. G. Larsson, and T. L. Marzetta, “Cell-free massive mimo: Uniformly great service for everyone,” in *2015 IEEE 16th International Workshop on Signal Processing Advances in Wireless Communications (SPAWC)*, 2015, pp. 201–205.
- [3] WG1: Use Cases and Overall Architecture Workgroup, *O-RAN Architecture-Description 6.0*, O-RAN Alliance Std., March 2022, version 6.0.
- [4] O. Orhan, V. N. Swamy, T. Tetzlaff, M. Nassar, H. Nikopour, and S. Talwar, “Connection management xapp for o-ran ric: A graph neural network and reinforcement learning approach,” in *2021 20th IEEE International Conference on Machine Learning and Applications (ICMLA)*, Dec 2021, p. 936–941.
- [5] M. Polese, L. Bonati, S. D’Oro, S. Basagni, and T. Melodia, “Understanding o-ran: Architecture, interfaces, algorithms, security, and research challenges,” *arXiv:2202.01032v2 [cs, eess]*, Aug 2022, arXiv: 2202.01032. [Online]. Available: <http://arxiv.org/abs/2202.01032>
- [6] H. A. Ammar, R. Adve, S. Shahbazpanahi, G. Boudreau, and K. V. Srinivas, “User-centric cell-free massive mimo networks: A survey of opportunities, challenges and solutions,” *IEEE Communications Surveys & Tutorials*, vol. 24, no. 1, p. 611–652, 2022.
- [7] S. Chen, J. Zhang, J. Zhang, E. Björnson, and B. Ai, “A survey on user-centric cell-free massive mimo systems,” *Digital Communications and Networks*, 2021.
- [8] S. Elhoushy, M. Ibrahim, and W. Hamouda, “Cell-free massive mimo: A survey,” *IEEE Communications Surveys & Tutorials*, vol. 24, no. 1, p. 492–523, 2022.

- [9] Ö. T. Demir, M. Masoudi, E. Björnson, and C. Cavdar, “Cell-free massive mimo in virtualized cran: How to minimize the total network power?” no. arXiv:2202.09254, Feb 2022, arXiv:2202.09254 [cs, eess, math]. [Online]. Available: <http://arxiv.org/abs/2202.09254>
- [10] R. Fantini, W. Zirwas, L. Thiele, D. Aziz, P. Baracca, M. Dohler, and T. Nakamura, *Coordinated multi-point transmission in 5G*. Cambridge University Press, 2016, p. 248–276.
- [11] G. Interdonato, E. Björnson, H. Quoc Ngo, P. Frenger, and E. G. Larsson, “Ubiquitous cell-free massive mimo communications,” *EURASIP Journal on Wireless Communications and Networking*, vol. 2019, no. 1, p. 197, Dec 2019.
- [12] S. Bassoy, H. Farooq, M. A. Imran, and A. Imran, “Coordinated multi-point clustering schemes: A survey,” *IEEE Communications Surveys & Tutorials*, vol. 19, no. 2, p. 743–764, 2017.
- [13] E. Björnson and L. Sanguinetti, “Scalable cell-free massive mimo systems,” *IEEE Transactions on Communications*, vol. 68, no. 7, p. 4247–4261, Jul 2020.
- [14] G. Interdonato, P. Frenger, and E. G. Larsson, “Scalability aspects of cell-free massive mimo,” in *ICC 2019 - 2019 IEEE International Conference on Communications (ICC)*, May 2019, p. 1–6.
- [15] F. Li, Q. Sun, X. Ji, and X. Chen, “Scalable cell-free massive mimo with multiple cpus,” *Mathematics*, vol. 10, no. 11, p. 1900, Jun 2022.
- [16] F. Riera-Palou and G. Femenias, “Decentralization issues in cell-free massive mimo networks with zero-forcing precoding,” in *2019 57th Annual Allerton Conference on Communication, Control, and Computing (Allerton)*, Sep 2019, p. 521–527.
- [17] J. Zheng, J. Zhang, E. Björnson, and B. Ai, “Impact of channel aging on cell-free massive mimo over spatially correlated channels,” *IEEE Transactions on Wireless Communications*, vol. 20, no. 10, p. 6451–6466, Oct 2021.
- [18] R. Chopra, C. R. Murthy, and A. K. Papazafeiropoulos, “Uplink performance analysis of cell-free mmimo systems under channel aging,” *IEEE Communications Letters*, vol. 25, no. 7, p. 2206–2210, Jul 2021.
- [19] J. Zheng, J. Zhang, E. Shi, J. Jiang, and B. Ai, “Uplink performance of high-mobility cell-free massive mimo-ofdm systems,” no. arXiv:2201.09622, Jan 2022, arXiv:2201.09622 [cs, eess, math]. [Online]. Available: <http://arxiv.org/abs/2201.09622>
- [20] A. Anand, C. R. Murthy, and R. Chopra, “Impact of mobility on downlink cell-free massive mimo systems,” no. arXiv:2209.02777, Sep 2022, arXiv:2209.02777 [cs, eess, math]. [Online]. Available: <http://arxiv.org/abs/2209.02777>
- [21] C. D’Andrea, G. Interdonato, and S. Buzzi, “User-centric handover in mmwave cell-free massive mimo with user mobility,” in *2021 29th European Signal Processing Conference (EUSIPCO)*, Aug 2021, p. 1–5.
- [22] Y. Xiao, P. Mähönen, and L. Simić, “Mobility performance analysis of scalable cell-free massive mimo,” no. arXiv:2202.01488, Feb 2022, arXiv:2202.01488 [cs, math]. [Online]. Available: <http://arxiv.org/abs/2202.01488>
- [23] M. Zaher, E. Björnson, and M. Petrova, “Soft handover procedures in mmwave cell-free massive mimo networks,” no. arXiv:2209.02548, Sep 2022, arXiv:2209.02548 [eess]. [Online]. Available: <http://arxiv.org/abs/2209.02548>
- [24] J. Wu, Z. Zhang, Y. Hong, and Y. Wen, “Cloud radio access network (c-ran): a primer,” *IEEE Network*, vol. 29, no. 1, p. 35–41, Jan 2015.
- [25] V. Q. Rodriguez, F. Guillemin, A. Ferrieux, and L. Thomas, “Cloud-ran functional split for an efficient fronthaul network,” in *2020 International Wireless Communications and Mobile Computing (IWCMC)*. Limassol, Cyprus: IEEE, Jun 2020, p. 245–250. [Online]. Available: <https://ieeexplore.ieee.org/document/9148093>
- [26] L. M. P. Larsen, A. Checko, and H. L. Christiansen, “A survey of the functional splits proposed for 5g mobile crosshaul networks,” *IEEE Communications Surveys & Tutorials*, vol. 21, no. 1, p. 146–172, 2019.
- [27] A. Checko, H. L. Christiansen, Y. Yan, L. Scolari, G. Kardaras, M. S. Berger, and L. Dittmann, “Cloud ran for mobile networks—a technology overview,” *IEEE Communications Surveys & Tutorials*, vol. 17, no. 1, p. 405–426, 2015.

- [28] E. Nayebi, A. Ashikhmin, T. L. Marzetta, and B. D. Rao, "Performance of cell-free massive mimo systems with mmse and lsfd receivers," in *2016 50th Asilomar Conference on Signals, Systems and Computers*, Nov 2016, p. 203–207.
- [29] H. Q. Ngo, A. Ashikhmin, H. Yang, E. G. Larsson, and T. L. Marzetta, "Cell-free massive mimo versus small cells," *IEEE Transactions on Wireless Communications*, vol. 16, no. 3, pp. 1834–1850, 2017.
- [30] E. Björnson and L. Sanguinetti, "Making cell-free massive mimo competitive with mmse processing and centralized implementation," *IEEE Transactions on Wireless Communications*, vol. 19, no. 1, pp. 77–90, 2019.
- [31] V. Ranjbar, A. Girycki, M. A. Rahman, S. Pollin, M. Moonen, and E. Vinogradov, "Cell-free mmimo support in the o-ran architecture: A phy layer perspective for 5g and beyond networks," *IEEE Communications Standards Magazine*, vol. 6, no. 1, p. 28–34, Mar 2022.
- [32] Ö. Özdogan, E. Björnson, and J. Zhang, "Performance of cell-free massive mimo with rician fading and phase shifts," *IEEE Transactions on Wireless Communications*, vol. 18, no. 11, p. 5299–5315, Nov 2019.
- [33] Y. Zhang, Q. Zhang, H. Hu, L. Yang, and H. Zhu, "Cell-free massive mimo systems with non-ideal hardware: Phase drifts and distortion noise," *IEEE Transactions on Vehicular Technology*, vol. 70, no. 11, p. 11604–11618, Nov 2021.
- [34] U. K. Ganesan, R. Sarvendranath, and E. G. Larsson, "Beamsync: Over-the-air carrier synchronization in distributed radioweeves," in *WSA 2021; 25th International ITG Workshop on Smart Antennas*. VDE, 2021, pp. 1–6.
- [35] O. T. Demir, E. Björnson, and L. Sanguinetti, "Cell-free massive mimo with large-scale fading decoding and dynamic cooperation clustering," in *WSA 2021; 25th International ITG Workshop on Smart Antennas*. VDE, 2021, pp. 1–6.
- [36] R. Beerten, A. Girycki, and S. Pollin, "User centric cell-free massive mimo in the o-ran architecture: Signalling and algorithm integration," in *2022 IEEE Conference on Standards for Communications and Networking (CSCN)*, pp. 181–187.
- [37] O. Y. Bursalioglu, G. Caire, R. K. Mungara, H. C. Papadopoulos, and C. Wang, "Fog massive mimo: A user-centric seamless hot-spot architecture," *IEEE Transactions on Wireless Communications*, vol. 18, no. 1, p. 559–574, Jan 2019.
- [38] Ö. T. Demir, E. Björnson, and L. Sanguinetti, "Foundations of user-centric cell-free massive mimo," *Foundations and Trends® in Signal Processing*, vol. 14, no. 3-4, pp. 162–472, 2021. [Online]. Available: <http://dx.doi.org/10.1561/2000000109>
- [39] V. Ranjbar, M. Moonen, and S. Pollin, "Local uplink processing in cell-free networks: A new approach," in *2021 29th European Signal Processing Conference (EUSIPCO)*, Aug 2021, p. 1616–1620.
- [40] J. Jose, A. Ashikhmin, T. L. Marzetta, and S. Vishwanath, "Pilot contamination and precoding in multi-cell tdd systems," *IEEE Transactions on Wireless Communications*, vol. 10, no. 8, p. 2640–2651, Aug 2011.
- [41] O-RAN WG4: Open Fronthaul Interfaces Workgroup, *O-RAN Control, User and Synchronization Plane Specification 9.0*, O-RAN Alliance Std., July 2022, version 9.0.
- [42] Z. Wang, E. Tameh, and A. Nix, "Joint shadowing process in urban peer-to-peer radio channels," *IEEE Transactions on Vehicular Technology*, vol. 57, no. 1, p. 52–64, Jan 2008.
- [43] R. He, Z. Zhong, B. Ai, and C. Oestges, "Shadow fading correlation in high-speed railway environments," *IEEE Transactions on Vehicular Technology*, vol. 64, no. 7, p. 2762–2772, Jul 2015.
- [44] E. Björnson, J. Hoydis, and L. Sanguinetti, "Massive MIMO networks: Spectral, energy, and hardware efficiency," *Foundations and Trends® in Signal Processing*, vol. 11, no. 3-4, pp. 154–655, 2017. [Online]. Available: <http://dx.doi.org/10.1561/2000000093>
- [45] G. Interdonato, H. Q. Ngo, P. Frenger, and E. G. Larsson, "Downlink training in cell-free massive mimo: A blessing in disguise," *IEEE Transactions on Wireless Communications*, vol. 18, no. 11, p. 5153–5169, Nov 2019, arXiv: 1903.10046.
- [46] WG3: Near-real-time RIC and E2 Interface Workgroup, *O-RAN Near-Real-time RAN Intelligent Controller Architecture & E2 General Aspects and Principles*, O-RAN Alliance Std., July 2022, version 2.02.